# Analysis of spatial assembly of GPCRs using photoactivatable dyes and localization microscopy

Kim C Jonas[1,2,3*] and Aylin C Hanyaloglu[3]

1. Molecular and Clinical Sciences Research Institute, St George's University of London, Cramner Terrace, London SW17 0RE.

2. Institute of Medical and Biomedical Education, St George's University of London, Cramner Terrace, London SW17 0RE, UK.

3. Institute of Reproductive and Developmental Biology, Imperial College London, Du Cane Road, London, W12 0NN, UK.

* Corresponding author, Email: kjonas@sgul.ac.uk.

**Running head:** Super resolution imaging of GPCR heteromers

**Key words:** G protein-coupled receptor, dimer, oligomer, heteromer, homomer, PD-PALM, super-resolution microscopy.

**Abstract**

Super-resolution imaging has provided unprecedented insight in the molecular complexities of fundamental cell biological questions. For G protein-coupled receptors (GPCRs), its application to the study of receptor homomers and heteromers have unveiled the diversity of complexes these GPCRs can form at the plasma membrane at a structural and functional level. Here we describe our methodological approach of photoactivated localization microscopy with photoactivable dyes (PD-PALM) to visualize and quantify the spatial assembly of GPCR heteromers at the plasma membrane.

## 1. Introduction

### *1.1 G protein-coupled receptor di/oligomerisation*

Developments in imaging technologies have contributed to our current understanding of the molecular regulation of G protein-coupled receptor (GPCR) activity. This is particularly pertinent for the study of receptor complexes, from GPCR engagement with its cognate G protein and key adaptor proteins such as arrestin, to GPCR-GPCR associations either as homomers or heteromeric complexes. Thus, techniques such as cryo-EM, single molecule tracking, fluorescence correlation spectroscopy and super-resolution imaging, have unveiled interaction interfaces, stoichiometry and single-molecule kinetics of these associations, particularly in the study of GPCR homo/heteromers**(1-6)**.

That GPCRs not only exist as monomers at the plasma membrane, but also as dimers and higher order oligomers has been reported for more than 20 years. Initially these studies employed classical biochemical approaches and then rapidly evolved with the advent of resonance energy transfer methods, particularly bioluminescence resonance energy transfer (BRET); enabling real time receptor-receptor interactions to be measured in intact cells **(7,8)**. However, the controversy in this area of GPCR biology has primarily stemmed from the cell systems used (heterologous cells overexpressing GPCRs) to the methodology themselves**(9-17)** this fruitful debate has facilitated the development of standardized methods and criteria in the study of GPCR homomers and particularly heteromers**(18)**. There have been numerous recent reports demonstrating physiologically relevant GPCR homomeric and heteromeric interactions, the transient and flexible nature of these associations and equally as important, that the propensity of certain GPCRs to associate as dimers or oligomers are likely to be receptor specific**(19-21)**.

We and others have previously described distinct single-molecule imaging modalities used to study GPCRs, and the advantages and limitations of each of these methods. Thus, we refer the reader to the following previous reviews**(6,22)**. Here we will discuss our methodology of the super-resolution imaging technique of photoactivatable localisation microscopy (PALM) using photoactivatable dyes (PD-PALM), within the context of applying this technology to study GPCR heteromers and the reorganization of these complexes following ligand activation.

### *1.2 PD-PALM unveils spatial organization and stoichiometry of GPCR homo/heteromers*

The ability of PALM and PD-PALM to visualize single molecules with <10nm resolution, compared to diffraction limited approaches where the maximal resolution is 200nm, is based on the following properties of employing photoswitchable or photoactivatable fluorophores. These probes, which in the case of PD-PALM are photoactivatable dyes, remain in the dark state until they undergo an uncaging process following exposure to UV light. This enables these probes to then be excited by the appropriate fluorophore-defined wavelength but then are subsequently, and irreversibly, photobleached into the dark state. In order to resolve individual molecules at higher densities than diffraction-limited single-molecule approaches, these uncaging/activation/photobleaching steps are carried out in a stochastic manner and repeated until all fluorophores have been activated and bleached in to the dark state.

We have employed PD-PALM to study the organization of complexes between the gonadotrophin hormone Class A GPCRs, specifically luteinising hormone receptor (LHR) di/oligomers and LHR heteromers with follicle-stimulating hormone receptor (FSHR)**(23)**. Our prior studies, and reviews, in this area have discussed the physiological importance of these interactions to reproduction**(22-24)**. In brief, we have shown that by using distinct LHR ligand binding-deficient and signal-deficient mutants, which alone are non-functional, but when co-

expressed, can activate Gαs-adenylate cyclase-cAMP signalling (the primary G protein pathway for this receptor) via functional complementation. This activity via receptor di/oligomerization was able to rescue the infertile phenotype in LHR knockout male mice**(20)**. Subsequently PD-PALM was employed to identify the organizational cell surface landscape of the wildtype and mutant LHRs undergoing functional complementation, as it enabled us to use these mutants as tools to directly visualize the protomers responsible for binding ligand, and those that mediate signalling. Furthermore, PD-PALM enabled us to resolve single receptor protomers at expression levels equivalent to those previously reported *in vivo*, in contrast to single-molecule tracking approaches that require very low expression or labelling in order to image single molecules. Using this approach, we observed that multiple forms of these receptors were observed (monomer, dimer and various oligomeric forms) and that 'heteromers' of the two mutant receptors were organized in functionally asymmetric oligomers that favoured more active receptor complexes, i.e. trimers and tetramers with an excess of binding deficient (signal-able) receptor over the signalling-deficient (ligand-binding) mutant receptor. An additional application of the PALM imaging studies was the integration with molecular modelling approaches to identify possible LHR-LHR interfaces. Surprisingly, this suggested that multiple interfaces for distinct di/oligomers were predicted, and is consistent with the concept that these receptors form diverse physical and functional complexes in our study and more recently in work with distinct Class A GPCRs**(25-27)**.

Our more recently published studies employing PD-PALM to visualise heteromers of LHR and FSHR also provided further support that the complexes formed are highly diverse in arrangement and potentially that asymmetric complexes favour certain cellular signalling profiles**(23)**. Unlike our studies with LHR homomers, ligand activation of LHR induced a highly specific increase in the number of LHR/FSHR heterotetramers, and favouring an increase in the proportion of FSHR protomers within a single tetramer**(23)**. This demonstrates the intricate molecular detail that can be obtained with this method for protein interactions with this super-

resolution method. The next sections will cover the materials, methods and troubleshooting steps to consider when undertaking PD-PALM experiments.

## 2. Materials

### 2.1 Plasmids

N terminally FLAG-tagged LHR and N-terminally HA-tagged FSHR, both in pcDNA3.1 plasmids, as previously described**(23,28)**.

### 2.2 Cell lines and transfection

HEK293 cells stably expressing FLAG-LHR, generated as previously described**(23,28)**, with transient transfection of HA-FSHR (see **Note 1**).

### 2.3 Antibody labelling

1. CAGE 500 and CAGE 552 NH3 esters (Abberior GMBH).

2. HA.11 mouse clone 16B12 (Biolegend), and FLAG rabbit (Sigma Aldrich). Buffers utilized during labelling of HA.11 and FLAG antibodies with CAGE dyes were purchased from Sigma Aldrich and Sephadex purification columns from GE Healthcare (UK). The labelling protocol (see **Note 2**) and required materials are as prescribed by Abberior, in Section 2.1 of their 'Labelling protocols' information section, (Abberior GMBH, Germany, http://www.abberior.com/site/assets/files/1856/20120316-labeling_protocol.pdf).

### 2.4 Transient transfections and cell culture

1. OptiMEM and Lipofectamine 2000, both from Thermo Fisher.

2. 1.5ml microfuge tubes, 6 well cell TC plates, 8 well glass-bottom chamberslides (#1.5, LabTech)

3. DMEM, 10% fetal bovine serum, 100iU/0.1mg penicillin/streptomycin, D-PBS and Trypsin.

4. 4% paraformaldehyde with 0.2% glutaraldehyde (4g in 100ml D-PBS). Weigh paraformaldehyde using a mask to minimize exposure, and heat to 50-60°C in a fume hood until dissolved. Leave to cool, check pH to ensure it is between 7.2-7.4, and add glutaraldehyde solution.

5. D-PBS with 1% sodium azide.

## 3. Methods

### *3.1 Transfection of receptors for PD-PALM studies*

Our transfection protocols were as follows:

1. Plate HEK293 cells stably expressing LHR into 1 X 35mm well to ensure a confluency of 80-90% the following day. We tend to plate using confluency rather than cell counts, but typically ~400,000 cells would achieve this.
2. The following day, check cells for confluency. If >90% confluent or <70%, it is not advisable to proceed with the transfection, as transfection efficiency will be compromised.
3. Using 2 separate 1.5ml microfuge tubes, prepare HA-FSHR plasmid DNA in OptiMEM and lipofectamine 2000 in OptiMEM (see **Table 1**), and incubate at RT for 5 minutes.
4. Combine the two OptiMEM DNA and lipofectamine 2000 containing solutions, and gently mix. Incubate at room temperature for a further 5 minutes.
5. Carefully add the OptiMEM-Lipofectamine 2000-DNA mix to the cells in a dropwise motion, and incubate at 37°C.
6. The following day, harvest the cells from the well, and re-plate into an 8-well glass-bottomed chamber slide and incubate overnight at 37°C (see **Note 3**).
7. Following overnight incubation, dilute CAGE 552-HA and CAGE-500-FLAG antibodies (we use 1:500) in 10% serum containing culture media (see **Note 4**)

8. From this point onwards, it is essential to switch the light off of the Class II cabinet and carry out the following steps in a darkened environment, to minimize any photoactivation of the CAGE dyes and preserve as much signal as possible.

9. Aspirate the media from cells and replace with CAGE-labelled antibody containing media and incubate at 37°C for 30 minutes.

10. Use ~300μl of antibody-media per well, but if the antibody were particularly precious, ~200μl would be sufficient.

11. During this time, prepare working concentrations of ligands in cell culture media. For our studies, we use LH and FSH at a concentration of 10-100nM.

12. At the end of the 30-minute incubation, aspirate media, carefully wash cells using D-PBS (containing calcium) and stimulate with ligand for desired time. For our studies, we tend to utilize a combination of time points, from very acute (30 seconds), to longer time points of 2 and 5 minutes.

13. Following stimulation, aspirate the media, wash cells twice in D-PBS, and fix for 30 minutes in 4% paraformaldehyde/0.02% glutaraldehyde (see **Note 5**). Again, use ~300μl of fixative, to ensure efficient fixation and a sufficient ratio of fixative to cell surface area.

14. Wash cells three times in D-PBS, and add 300μl of D-PBS containing 1% sodium azide, to prevent growth of bacteria, etc. Store at 2-8°C, in darkness (using a light-controlled box and foil) until imaged. We typically image within 24-72 hours of labelling.

### *3.2 PD-PALM image acquisition*

For our previous work, we have utilized a custom-made super resolution adapted total-internal reflection fluorescence (TIRF) microscope, the specification of which is previously described**(22,24)**. For our more recent studies, we have moved to a commercially available microscope, the Zeiss Elyra PS1 (Zeiss, Germany), a somewhat more user-friendly and automated microscopy platform. Both have their merits and downsides, however, for the purpose of this Chapter, we will describe our imaging methods using the commercially

available Elyra microscope. The principles of acquiring and resolving single GPCR molecules are the same, whichever platform used. The Elyra microscope we used, was custom designed to enable simultaneous dual-colour imaging, via the provision of an additional EM-CCD camera (two cameras in total, one per fluorophore). Should only one camera be available, sequential imaging of differential fluorophores with each frame will be required. In terms of other technical set-up points, the microscope is surrounded by a temperature controlled, dark-box, for maximizing stabilization of the imaging environment and preventing light exposure (both to sample, and from exposure to high laser power to the user). The lasers that we utilized have the following power capabilities; 405nm -50mW, 488nm- 200mW and 561nm- 200mW. The imaging of single GPCR molecules is somewhat difficult to describe a set protocol for. However, below is an approximate 'how-to' with tips and pointers that we have found useful through our imaging endeavours (see **Figure 1** for additional trouble shooting guide):

1. Open the Zen software and ensure two camera imaging is selected.
2. Turn on the UV (405nm), 488nm and 561nm laser lines and allow to warm up and stabilize for 30 minutes.
3. Set up the following image parameters: TIRF mode, X100 objective, a time-lapse series (we typically use 10,000 frame imaging at 10 frames/second) with simultaneous imaging using 405 and detection within green and red excitation/emission spectra. The size of your imaging area is also something to consider- the larger this is, the larger your file size. We typically image a 256 X 256 pixel area.
4. Clean the X100 1.4NA objective using microscope tissue and 70% ethanol and add a drop of emersion oil to the lens. Be sure to allow the 70% ethanol to fully evaporate from the lens, and also to use emersion oil with the correct refractive index for D-PBS.
5. Place the chamber slide onto the microscope and using the locate function tab in the Zen software, scroll through the Z plane to locate the cells.

6. Once cells are located, using minimal UV and low power of 488nm and 561nm laser lines, use a combination of adjusting the focal plane, and TIRF angle until distinct activated fluorophores are detected.

7. At this point, switch on the definite focus function to minimize drift, and increase UV, 488 and 561 laser powers to achieve sufficient activation of spatially separate fluorophores. Having spatially separate fluorophores is imperative to being able to localize individual receptor molecules, so is very important. The selection of laser power is a delicate balance between achieving sufficient photoactivation and efficient photobleaching, and thus will vary dependent on fluorophores used, system set and sensitivity of the camera, so it is difficult to be prescriptive with exact laser settings.

8. Whilst imaging is occurring, you can monitor the localization events within the analysis part of the Zen software. This acts as a good guide for quality of the imaging and for laser settings in terms of effectiveness of photobleaching.

### 3.3. *Extracting xy coordinates from acquired PD-PALM movies*

For obtaining xy coordinates download the freely available, open source Fiji imaging software and QuickPALM plug-in**(29)**:

1. Open .zsi image file obtained from Zeiss Elyra in Fiji.

2. Adjust brightness of image to visualize your activated fluorophores and delete any frames from the beginning of the movie where initial adjustments were made.

3. Separate the movie in to two channels; within the ‘Image’ tab, go to ‘Color’ and ‘Split channels’. This will allow the two receptors to be separately analysed.

4. Create 7x7 uM squares within the cell boundaries.

5. Create a separate sub-stack under Image tab and Duplicate function, making sure to select the box for sub-stack.

6. Select quickPALM function within Plugins tab.

7. Within the dropdown menu enter the pixel size, which is obtainable from each individual image on the Zeiss Zen software, the full width half maximum of the individual localized fluorophores, and the signal to noise ratio (see **Note 6**).

8. Run the analysis and save the generated .csv *xy* coordinates file. You can also save the image generated alongside this.

9. Repeat the process for the second channel and for other cells within the image (see **Note 7**).

### 3.4. *Quantitation of GPCR complexes via PD-Interpreter*

For quantitation of GPCR complexes we designed a custom Java-based software package designed to analyse localisation microscopy super resolution data called PD-Interpreter. PD-interpreter utilises the localisation co-ordinates generated (as described in Section 3.3), to analyse the number of monomers/dimers/oligomers for 2-channel acquired PALM data. The software analysis is based on a model proposed by Getis and Franklin, which uses a modified $2^{nd}$ order neighbourhood analysis approach (see **Note 8**).

1. Download PD-interpreter from www.superimaging.org.

2. Open program and select the parameters tab.

3. Select the desired radius for analysis denoted as spatial scale (default =10nm yet ranges to 1000nm). For LHR and FSHR we have used 50nm (see **Note 9**).

4. Select the file tab and load the first channel of the data set into ‘load right data set’, remembering which wavelength this channel data represents.

5. Select the file tab and load the second channel of the data set into ‘load left data set’.

6. Select the ‘analyse’ tab and ‘calculate clusters’ command. The progress of the analysis can be monitored using the live updating bar at the bottom of the page. The analysis is complete when this bar states ‘got left/right clusters’.

**7.** Once completed, select the ‘analyse’ tab and ‘output cluster data’. Selecting this will save the folder containing all data (Excel spreadsheet with localisation data and

accompanying images) into the folder from which the original data sets were obtained. The PD-Interpreter folder will be saved with the date and time of the analysis (see **Note 10**).

8. To continue analysing more data sets, select 'file', 'reset'. Further localisation data sets can then be loaded and analysed. The radius set in step 2 will remain at your chosen setting until the program is closed. The Excel spreadsheets contain a summary page with total self-associating and co-associating molecules and from which the monomer population can be obtained. A breakdown of the number of each complex type (dimer, trimer etc, and labelled as 2, 3, etc in the Summary tab) is also provided. For heteromers, the number of protomers within each individual complex is also detailed within this summary page. Additional tabs contain the individual *xy* coordinates of each assigned self-associating and co-associating complexes, and non-associating molecules. Data is also outputted as several different individual image files, initially depicting all molecules in the localisation data sets from the 2 channels. From the analysis, co-localisation plots are generated using blue and yellow colours to differentiate the two channel populations, and a multi-colour plot depicting complex sizes and representing clusters with 2 or more molecules in represented by different colours (both omitting non-associating molecules).

## 4. Notes

1. Before beginning our PD-PALM experiments, the amount of HA-FSHR plasmid transfected was firstly optimized to ensure we could detect FSHR expression at the cell surface, and for effects on FSH and LH-dependent cAMP production. Our transfection reagent of preference is Lipofectamine 2000 (Invitrogen). We find that this gives a good transfection efficiency- typically 60-70% of cells and has very low toxicity to the cells.

2. To quantitate individual GPCR molecules, it is essential to have a 1:1 labelling of CAGE dye:antibody. Both the FSHR and LHR were differentially N-terminally tagged with small epitopes, namely HA and FLAG, respectively, therefore we utilized HA and FLAG antibodies for our studies. The choice of CAGE dyes is an important factor to consider, when wanting to label and visualize two different receptor subtypes, as the dyes will need to be

spectrally separate to minimize bleed through between channels. The CAGE dyes we utilized are CAGE 500 and CAGE 552, detected by 488nm and 561nm laser lines, respectively, with spectral properties that are sufficiently separate to ensure specificity of detection. The CAGE dyes are available in a number of different modified forms from the manufacturer e.g., malamide or NH3 ester. For our studies, we utilized the NH3 ester label and differentially labelled the HA.11 and FLAG antibodies follow the step-by-step guide provided by the manufacturer's, thus we will not describe this in detail here. An important factor for achieving a 1:1 ratio of CAGE dye:antibody is the molar ratio of label:antibody used. For this, we used a ratio of 1:10, which in our hands with our antibodies was sufficient to achieve a labelling density of 1.3 ± 0.1 for HA-CAGE 552, and 1.0 ± 0.2 for FLAG-CAGE 500. Labelling efficiency was determined, again following manufacturer's instructions, by employing a derivate of the Beer-Lambert Law.

3. We routinely use 60% of the harvested cells to re-plate into the chamber slides, to achieve a confluency of approximately 50-60%. This ensures cells are a distinct monolayer, and not too confluent to image. Incubate overnight at 37°C.

4. When optimizing our labelling conditions, we trialled many blocking agents. A comprehensive discussion of this can be found elsewhere**(22)**.

5. The addition of glutaraldehyde is important as it has been shown to minimize lateral diffusion of transmembrane proteins, that cross-linking reagents such as paraformaldehyde, have been previously shown to fail to prevent**(30,31)**.

6. For a description of how to calculate the full width half maximum and signal to noise ratio values, please refer to our previous publications**(22,24)**.

7. Filter any fluorophores that have remained on for multiple frames due to inefficient bleaching via the Zen software (during image acquisition) or via freely-available ImageJ plugin ThunderSTORM.

8. This model determines if two (or more) molecules are located within a defined search radius, if so, they are identified as interacting, ultimately assessing the association and localisation patterns of molecules of interest**(32)**.

9. We utilise a 50nm radius based on the size of the large extracellular domain of the gonadotrophin receptors, the size of the antibody, and localisation precision.

10. It is essential to save the output data after each run, or data will not be saved.

## 5. References


1. Liang YL, Khoshouei M, Radjainia M, Zhang Y, Glukhova A, Tarrasch J, Thal DM, Furness SGB, Christopoulos G, Coudrat T, Danev R, Baumeister W, Miller LJ, Christopoulos A, Kobilka BK, Wootten D, Skiniotis G, Sexton PM. Phase-plate cryo-EM structure of a class B GPCR-G-protein complex. Nature. 2017;546(7656):118-123.

2. Baidya M, Dwivedi H, Shukla AK. Frozen in action: cryo-EM structure of a GPCR-G-protein complex. Nat Struct Mol Biol. 2017;24(6):500-502.

3. Mayer JP, Tschöp MH, DiMarchi RD. Once Blind, Now We See GLP-1 Molecular Action. Cell Metab. 2017;26(2):289-291.

4. Martínez-Muñoz L, Rodríguez-Frade JM, Barroso R, Sorzano CS, Torreño-Pina JA, Santiago CA, Manzo C, Lucas P, García-Cuesta EM, Gutierrez E, Barrio L, Vargas J, Cascio G, Carrasco YR, Sánchez-Madrid F, García-Parajo MF, Mellado M. Separating Actin-Dependent Chemokine Receptor Nanoclustering from Dimerization Indicates a Role for Clustering in CXCR4 Signaling and Function. Mol Cell. 2018;70(1):106-119.e110.

5. Briddon SJ, Kilpatrick LE, Hill SJ. Studying GPCR Pharmacology in Membrane Microdomains: Fluorescence Correlation Spectroscopy Comes of Age. Trends Pharmacol Sci. 2018;39(2):158-174.

6. Scarselli M, Annibale P, McCormick PJ, Kolachalam S, Aringhieri S, Radenovic A, Corsini GU, Maggio R. Revealing G-protein-coupled receptor oligomerization at the single-molecule level through a nanoscopic lens: methods, dynamics and biological function. FEBS J. 2016;283(7):1197-1217.

7. Pfleger KD, Eidne KA. Monitoring the formation of dynamic G-protein-coupled receptor-protein complexes in living cells. Biochem J. 2005;385(Pt 3):625-637.

8. Milligan G, Ramsay D, Pascal G, Carrillo JJ. GPCR dimerisation. Life Sci. 2003;74(2-3):181-188.

9. Bouvier M, Heveker N, Jockers R, Marullo S, Milligan G. BRET analysis of GPCR oligomerization: newer does not mean better. Nat Methods. 2007;4(1):3-4; author reply 4.

10. Bouvier M, Hébert TE. CrossTalk proposal: Weighing the evidence for Class A GPCR dimers, the evidence favours dimers. J Physiol. 2014;592(12):2439-2441.

11. Bouvier M, Hébert TE. Rebuttal from Michel Bouvier and Terence E. Hébert. J Physiol. 2014;592(12):2447.

12. Lambert NA, Javitch JA. CrossTalk opposing view: Weighing the evidence for class A GPCR dimers, the jury is still out. J Physiol. 2014;592(12):2443-2445.

13. Lambert NA, Javitch JA. Rebuttal from Nevin A. Lambert and Jonathan A. Javitch. J Physiol. 2014;592(12):2449.

14. Chabre M, le Maire M. Monomeric G-protein-coupled receptor as a functional unit. Biochemistry. 2005;44(27):9395-9403.

15. James JR, Oliveira MI, Carmo AM, Iaboni A, Davis SJ. A rigorous experimental framework for detecting protein oligomerization using bioluminescence resonance energy transfer. Nat Methods. 2006;3(12):1001-1006.

16. Fotiadis D, Jastrzebska B, Philippsen A, Müller DJ, Palczewski K, Engel A. Structure of the rhodopsin dimer: a working model for G-protein-coupled receptors. Curr Opin Struct Biol. 2006;16(2):252-259.

17. Salahpour A, Masri B. Experimental challenge to a 'rigorous' BRET analysis of GPCR oligomerization. Nat Methods. 2007;4(8):599-600; author reply 601.

18. Kenakin T, Agnati LF, Caron M, Fredholm B, Guidoli D, Kobilka B, Lefkowitz RW, Lohse M, Woods A, Fuxe K. International Workshop at the Nobel Forum, Karolinska Institutet on G protein-coupled receptors: finding the words to describe monomers, oligomers, and their molecular mechanisms and defining their meaning. Can a consensus be reached? J Recept Signal Transduct Res. 2010;30(5):284-286.

19. Albizu L, Cottet M, Kralikova M, Stoev S, Seyer R, Brabet I, Roux T, Bazin H, Bourrier E, Lamarque L, Breton C, Rives ML, Newman A, Javitch J, Trinquet E, Manning M, Pin JP, Mouillac B, Durroux T. Time-resolved FRET between GPCR ligands reveals oligomers in native tissues. Nat Chem Biol. 2010;6(8):587-594.

20. Rivero-Müller A, Chou YY, Ji I, Lajic S, Hanyaloglu AC, Jonas K, Rahman N, Ji TH, Huhtaniemi I. Rescue of defective G protein-coupled receptor function in vivo by intermolecular cooperation. Proc Natl Acad Sci U S A. 2010;107(5):2319-2324.

21. Viñals X, Moreno E, Lanfumey L, Cordomí A, Pastor A, de La Torre R, Gasperini P, Navarro G, Howell LA, Pardo L, Lluís C, Canela EI, McCormick PJ, Maldonado R, Robledo

P. Cognitive Impairment Induced by Delta9-tetrahydrocannabinol Occurs through Heteromers between Cannabinoid CB1 and Serotonin 5-HT2A Receptors. PLoS Biol. 2015;13(7):e1002194.

22. Jonas KC, Huhtaniemi I, Hanyaloglu AC. Single-molecule resolution of G protein-coupled receptor (GPCR) complexes. Methods Cell Biol. 2016;132:55-72.

23. Jonas KC, Chen S, Virta M, Mora J, Franks S, Huhtaniemi I, Hanyaloglu AC. Temporal reprogramming of calcium signalling via crosstalk of gonadotrophin receptors that associate as functionally asymmetric heteromers. Sci Rep. 2018;8(1):2239.

24. Jonas KC, Fanelli F, Huhtaniemi IT, Hanyaloglu AC. Single molecule analysis of functionally asymmetric G protein-coupled receptor (GPCR) oligomers reveals diverse spatial and structural assemblies. J Biol Chem. 2015;290(7):3875-3892.

25. Martínez-Muñoz L, Barroso R, Dyrhaug SY, Navarro G, Lucas P, Soriano SF, Vega B, Costas C, Muñoz-Fernández M, Santiago C, Rodríguez Frade JM, Franco R, Mellado M. CCR5/CD4/CXCR4 oligomerization prevents HIV-1 gp120IIIB binding to the cell surface. Proc Natl Acad Sci U S A. 2014;111(19):E1960-1969.

26. Jin J, Momboisse F, Boncompain G, Koensgen F, Zhou Z, Cordeiro N, Arenzana-Seisdedos F, Perez F, Lagane B, Kellenberger E, Brelot A. CCR5 adopts three homodimeric conformations that control cell surface delivery. Sci Signal. 2018;11(529).

27. Dijkman PM, Castell OK, Goddard AD, Munoz-Garcia JC, de Graaf C, Wallace MI, Watts A. Dynamic tuneable G protein-coupled receptor monomer-dimer populations. Nat Commun. 2018;9(1):1710.

28. Jean-Alphonse F, Bowersox S, Chen S, Beard G, Puthenveedu MA, Hanyaloglu AC. Spatially restricted G protein-coupled receptor activity via divergent endocytic compartments. J Biol Chem. 2014;289(7):3960-3977.

29. Henriques R, Lelek M, Fornasiero EF, Valtorta F, Zimmer C, Mhlanga MM. QuickPALM: 3D real-time photoactivation nanoscopy image processing in ImageJ. Nat Methods. 2010;7(5):339-340.

30. Tanaka KA, Suzuki KG, Shirai YM, Shibutani ST, Miyahara MS, Tsuboi H, Yahara M, Yoshimura A, Mayor S, Fujiwara TK, Kusumi A. Membrane molecules mobile even after chemical fixation. Nat Methods. 2010;7(11):865-866.

31. Annibale P, Vanni S, Scarselli M, Rothlisberger U, Radenovic A. Identification of clustering artifacts in photoactivated localization microscopy. Nat Methods. 2011;8(7):527-528.

32. Rossy J, Cohen E, Gaus K, Owen DM. Method for co-cluster analysis in multichannel single-molecule localisation data. Histochem Cell Biol. 2014;141(6):605-612.

**Figure Legend**

**Figure 1. Trouble shooting guide for PD-PALM imaging.** Blue arrows depict the standard work flow of image acquisition for PD-PALM, detailing common issues experienced at each step of imaging (red arrows), and solutions to these problems (green arrows).

**Table Legend**

**Table 1. Lipofectamine 2000-mediated transfection conditions employed for transient transfection of FSHR.**

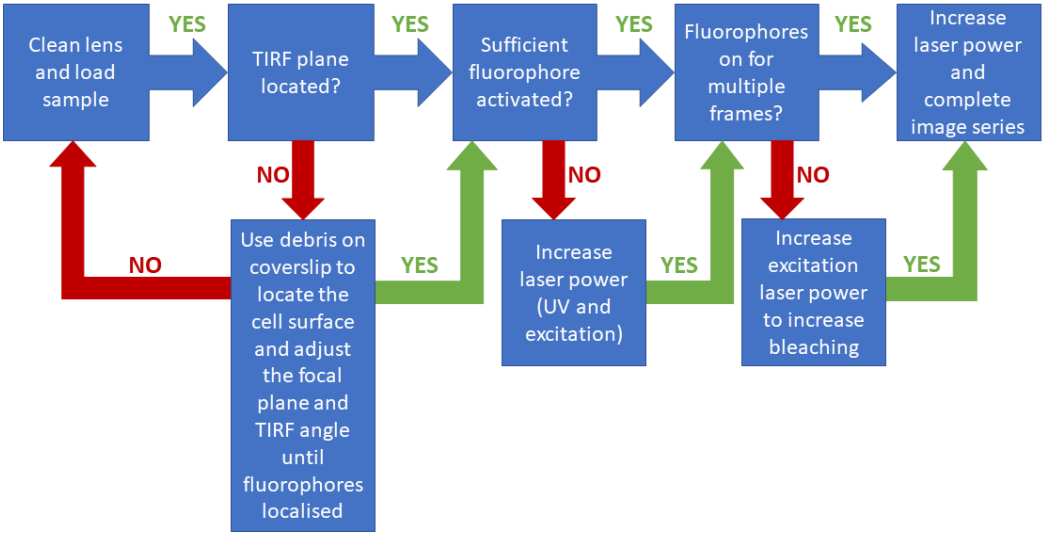


**Figure 1. Jonas and Hanyaloglu**

| Vol. Lipofectamine 2000 (μl) | Amount of FSHR DNA (μg) | Vol. of OptiMEM (μl) |
|---|---|---|
| 10 | | 125 |
| | 2.5 | 125 |

**Table 1. Jonas and Hanyaloglu**